Infrared On-orbit Inspection of Shuttle Orbiter Reinforced Carbon-Carbon Using Solar Heating

P. A. Howell, W. P. Winfree, and K. Elliott Cramer

MS 231, 3B E Taylor Rd
NASA Langley Research Center
Hampton, VA 23681

ABSTRACT

Thermographic nondestructive inspection techniques have been shown to provide quantitative, large area damage detection capabilities for the ground inspection of the reinforced carbon-carbon (RCC) used for the wing leading edge of the Shuttle orbiter. The method is non-contacting and able to inspect large areas in a relatively short inspection time. Thermal nondestructive evaluation (NDE) inspections have been shown to be applicable for several applications to the Shuttle in preparation for return to flight, including for inspection of RCC panels during impact testing, and for between-flight orbiter inspections.

The focus of this work is to expand the capabilities of the thermal NDE methodology to enable inspection by an astronaut during orbital conditions. The significant limitations of available resources, such as weight and power, and the impact of these limitations on the inspection technique are discussed, as well as the resultant impact on data analysis and processing algorithms. Of particular interest is the impact to the inspection technique resulting from the use of solar energy as a heat source, the effect on the measurements due to working in the vacuum of space, and the effect of changes in boundary conditions, such as radiation losses seen by the material, on the response of the RCC. The resultant effects on detectability limits are discussed.

Keywords: Nondestructive Evaluation, Shuttle, on-orbit inspection, thermography, infrared

1. INTRODUCTION

Following the loss of the Space Shuttle Columbia in February of 2003, the Columbia Accident Investigation Board (CAIB), an independent review board, was tasked to determine the cause of the accident and to suggest operational improvements for NASA's space program. The board made numerous suggestions for NASA to implement, two of which were that NASA:

> "Develop and implement a comprehensive inspection plan to determine the structural integrity of all Reinforced Carbon-Carbon system components. This inspection plan should take advantage of advanced nondestructive inspection technology." (CAIB recommendation: R3.3-1) [1]

and

> "… Accomplish an on-orbit Thermal Protection System inspection, using appropriate assets and capabilities, early in all missions. The ultimate objective should be a fully autonomous capability for all missions to address the possibility that an International Space Station mission fails to achieve the correct orbit, fails to dock successfully, or is damaged during or after undocking." (CAIB recommendation R6.4-1) [1]

This paper discusses the development of an on-orbit inspection system to detect subsurface damage to the Reinforced Carbon-carbon (RCC) components of the Orbiter. The technique leverages the thermal NDE technique used for ground inspection of the RCC, and this paper presents analyses of the technical challenges involved with advancing that technique to an orbital inspection system. The ground-based thermal NDE system was used extensively during impact testing of the RCC to provide real-time feedback to the impact test team regarding damage sustained during tests. In some cases, the availability of this data influenced real time modifications to the overall test matrix. Additionally, a

thermography system was developed to fully inspect the RCC between Shuttle missions. Details of these applications of Thermal NDE to the Shuttle's RCC materials can be found in [2] and [3].

2. OPERATIONAL CONCEPT

The development of inspection tools for the Orbiter's Thermal Protection System (TPS) was critical to NASA's Return-to-Flight efforts. A boom-mounted sensor system containing a 3D laser, the Laser Dynamic Range Imager (LDRI), and a visible camera will scan the TPS. Both instruments in the sensor package detect surface anomalies with a spatial resolution of a few millimeters. The boom mounted instruments can be used to inspect low-temperature reusable surface insulation (LRSI), high-temperature reusable surface insulation (HRSI) and RCC. Infrared thermography, on the other hand, is capable of detecting both surface and subsurface damage that could have been caused by an in-service event, such as delaminations, silicon-carbide coating loss, and surface cracks typically seen in the presence of subsurface delaminations. The additional benefits of infrared NDE for on-orbit inspection is that it is noncontacting and images large areas in a relatively short period of time, requiring access to only a single side of the structure.

The Shuttle Astronaut Crew Office established requirements for a hand-held system for inspecting the TPS, to be used during mission Extravehicular Activity, (EVA). This operational concept is illustrated in Figure 1 below.

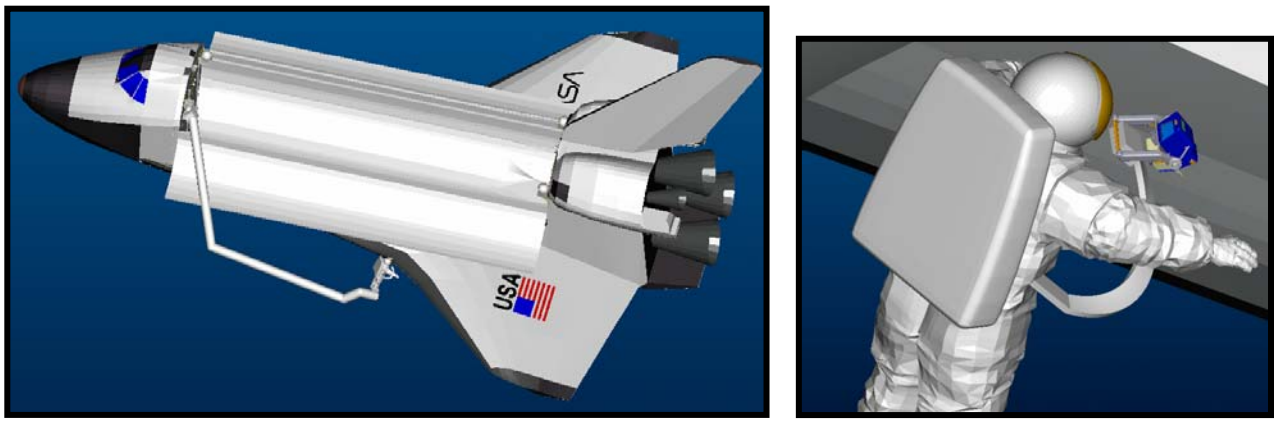

Figure 1. Operational concept: IR Inspection via astronaut EVA.

To provide an external heat source for the inspection, solar energy is used. This approach reduces the system weight, power, and development time requirements by avoiding the need for a secondary heat source, but places an operational constraint on the measurement as the data must necessarily be taken during the daylight portion of the orbit.

To assist in validating the performance of the infrared imager and inspection concept, an infrared system will be flown on two Shuttle missions: STS-121 and STS-155 and tested on a designed experiment, or DTO (Development Test Objective). The major objectives of this effort are (1) the development of an operational concept, (2) development of an infrared camera suitable for space operation, (3) transitioning the inspection technique and analysis software for orbital boundary conditions, (4) measurement of the thermal boundary conditions seen by the wing leading edge during orbit, and (5) inspection and characterization of damaged RCC samples during orbit. To meet the last objective, two RCC test articles will be flown on the two missions. The first test article contains four flat-bottom holes of 50% material loss from the back surface of the RCC sample and ranging in diameter from 1 inch to 2 inches. The second test article that will be imaged on-orbit was impacted with SOFI (Spray On Foam Insulation) to create true subsurface delaminations. Data from these test articles and the temperature history of the wing leading edge will assist in validation of ground analyses and models and provide a basis for development of an operational thermal NDE system with RCC damage detection capability with passive solar heating.

3. TRANSITIONING TO ORBITAL OPERATION

The significant limitations of available resources during space missions, such as weight and power, were defining parameters in the selection of the infrared camera. Further, budget and time considerations led to a decision to modify a commercial off the shelf (COTS) camera. This camera had to be capable of collecting and storing a series of images to provide the necessary data for NDE processing. Details of the camera modifications necessary to transition the COTS camera to space flight hardware are discussed in [4].

3.1. Camera choice for weight/ capability specifications

An uncooled microbolometer camera was chosen in order to minimize the system weight and required power. While cooled detector cameras provide significantly better signal-to-noise, the microbolometer provides sufficient signal-to-noise for detecting delaminations of the size and depth of interest, with lower weight and power consumption. The camera has a spectral range of 7.5 to 13µm with a 320 x 240 pixel focal plane array. The field of view is 24° x 18° with a minimum focus distance of 0.3m. It has a thermal sensitivity of 0.06°C at ambient and can collect and store up to 600 frames of 14 bit integer data to built-in RAM at a maximum frame rate of 60 Hz. After collecting the data in RAM, the camera can then write to a removable compact flash memory card. The flash memory card will be used to transfer the data to an onboard computer for transmission to the ground for processing.

3.2. Impact Panel Descriptions

Seven samples approximately 6” wide x 6” high of RCC material were impacted with SOFI foam as shown in Figure 2 [5]. All seven samples were cut from a previously flown section of RCC to provide samples with surface emissivity variations as seen on flight panels. The samples were held in a metal frame around the edge to allow the RCC to flex upon impact. The edges of the samples were cushioned from the metal frame with pliable putty to allow further sample motion. The RCC was impacted with SOFI foam that measured 1 inch x 1 inch in cross section and was 2 inches long with a weight of 2 grams. The panels were impacted at speeds of approximately 2000 ft/s.

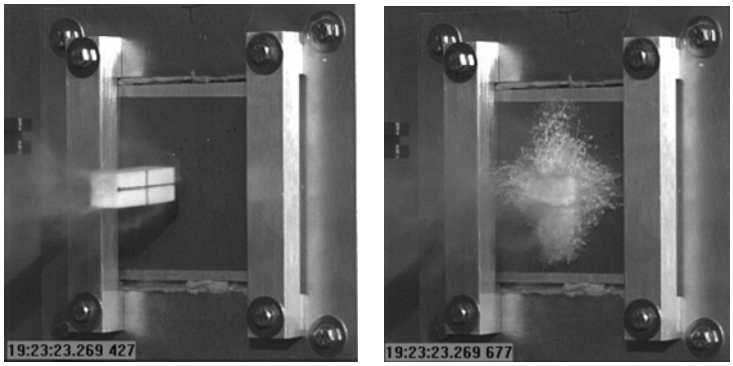

Figure 2. Impact of RCC with foam at approximately 2000 ft/s.

These seven impact panels (see Figure 3) provided samples with a range of realistic delaminations to be used for technique development. The samples were characterized with ground thermography, with both active and simulated solar heating and with both the ground-based IR camera (In-Sb) and a commercial version of the microbolometer camera chosen for the orbital IR camera. X-ray computed tomography data was also taken on all seven samples. Data that will be taken during the mission DTO will be compared to this ground-based data.

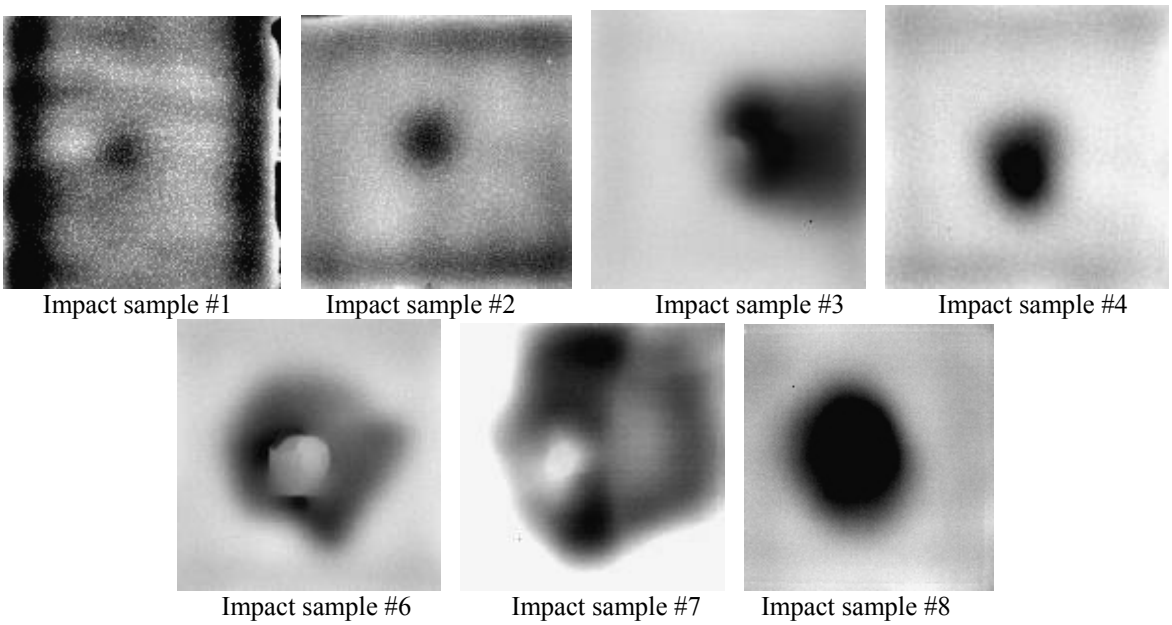

Figure 3. Processed flash thermography (baseline) data of seven impacted RCC samples. Delaminations from ½" in diameter (#1) to 4 ½" x 5 ½" (#7) (Note: impact sample #5 was removed from the test set prior to impact to be used in a different test)

3.3. Input Heat Flux

One of the technology requirements of transitioning the NDE technique to an orbital system is the adaptation of the input heat flux for in-space operations. For the ground-based system, a short flash of heat is delivered to the front surface of the sample via two 2400 J xeon flash lamps. The data is collected during the cool-down of the surface as shown in Figure 4a. Reliance on solar energy to provide the input heat flux results in a much slower application of heat, as shown in Figure 4b. The optimal data reduction requires a time varying thermal contrast between a flaw and an unflawed material, therefore the optimal data must be taken at the onset of solar heating or at the end of solar heating phase. Rather than relying on the orbital cycle to set the timing of the solar heating cycle, blocking the sun light controls the initiation and end of solar heat during data collection. Ground-based experiments showed the feasibility of this approach both from a crew operations perspective as well as a data analysis perspective. NDE results of data collected under solar conditions on RCC both with and without shading is shown in Figure 5.

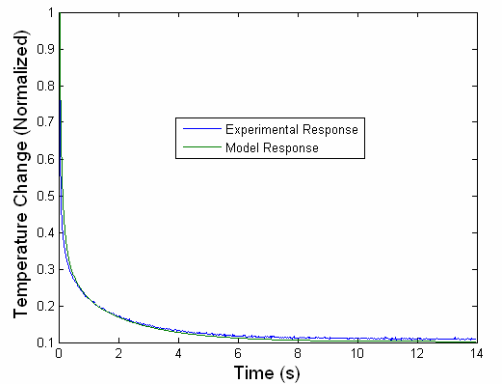

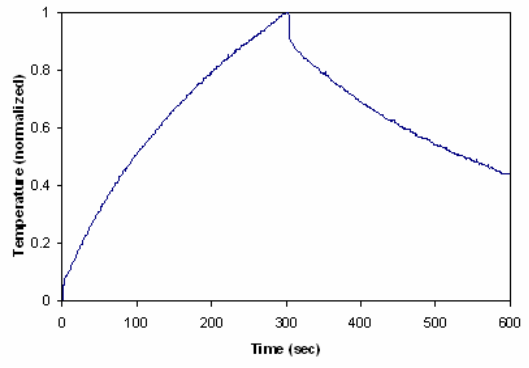

Figure 4. (A) Response of RCC to flash heat pulse (B) Response of RCC to solar heating at atmosphere with shading

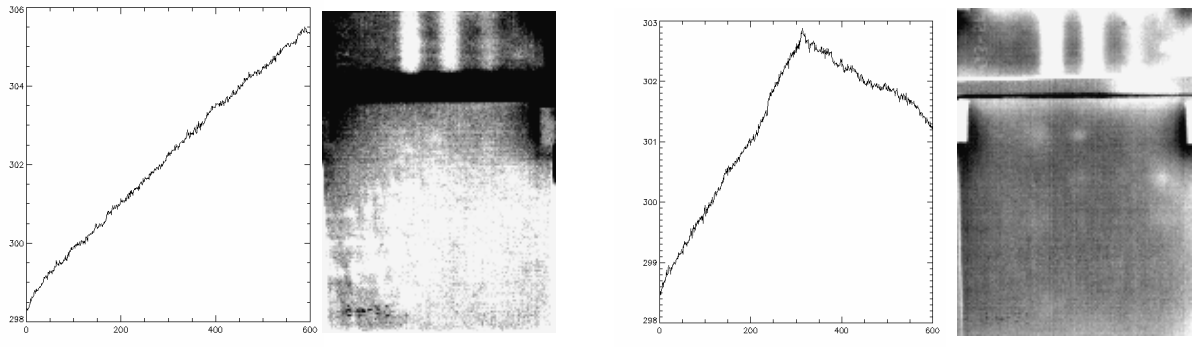

Figure 5. Processed thermal data on Shuttle RCC under solar conditions with no shading (a) and with shading (b)

3.4. Camera Focus

Unlike a visible camera, focus of an IR image for NDE applications is not critical. The contrast due to a subsurface defect does not have well defined edges, since the heat diffuses laterally within the structure. Therefore, the features of interest for detection of subsurface flaws can be obtained if the camera is slightly out of focus. For the camera chosen, the effect of poor focus on the NDE measurement was examined by setting the camera 3 feet away from the sample and establishing proper focus. With the focus setting unchanged, the separation between the camera and sample was varied, resulting in delamination indications that were out of focus. These results are shown below in Figure 6.- As can be seen in the figure, the image degradation is greatest when the separation is less than the set focal distance. The resultant effect on the NDE measurement is a lower amplitude contrast due to the defect and an indication with a larger area of damage than actually exists.

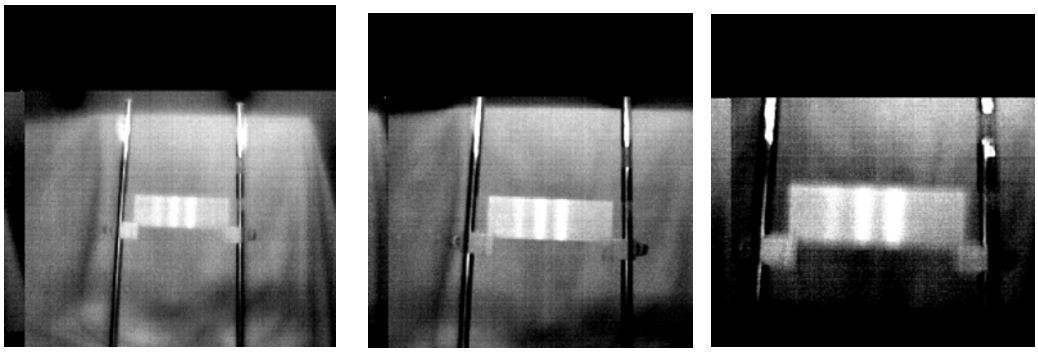

Figure 6. Camera located (A) 12 inches further away than actual focal distance setting from camera to target. (B) at actual focal distance setting from camera to target and (C) 12 inches closer than actual focal distance setting from camera to target.

Two approaches were implemented to provide camera focus on the RCC. First, several preset focal lengths can be chosen by the crew while on the EVA. Tests indicated that the crew was able to estimate the distance from the camera to the target within the applicable range. Second, the DTO calls for the crew to be 3 to 6 feet away from the WLE during data collection. At this distance, the T-seals between RCC panels are visible within the image. The T-seals have a larger thermal mass than the panels, therefore will typically have a surface temperature that is different from the panels. The temperature contrast between the panels and the T-seals enables the camera to be focused. Figure 7 illustrates the temperature contrast between the T-seal and panel under solar heating conditions.

Figure 7. (A) Photograph of WLE RCC and (B) Focus ability T-seals located between RCC panels during solar heating.

3.5. Data analysis: PCA

Principle Component Analysis (PCA) is an algorithm based on decomposition of the thermal data into its principle components. Singular value decomposition is a routine used to find the singular values and corresponding eigenvectors of a matrix. Since thermal NDE signals are well behaved and slowly decaying waveforms, the spatial variations of the entire data set is usually contained in the first and second eigenvectors and accounts for most of the data variance. The PCA is computed by defining a data matrix, A, where the time variations are along the columns and the spatial image pixel points are row-wise. The matrix A can then be decomposed as follows:

$$A = U * \Gamma * V^T$$

where Γ is the a diagonal matrix containing the singular values, V is an orthogonal matrix with dimensions corresponding to the number of images or time history, and U is an orthogonal matrix which contains the eigenvectors describing the spatial variations, and therefore, each column of U contains the eigenvectors which can be configured to generate the PCA image. Typically the first eigenvector PCA image provides good contrast for defect detection. PCA analyses were used routinely on the flash thermography conducted for ground inspections. It was found that PCA also works well for the longer heat pulse input flux condition, using approximately the first 10 seconds of data immediately after shadowing of the sample.

3.6. Increasing Signal-to-noise: Anistropic Diffusion

Anisotropic diffusion is a data processing technique that has been shown to enhance the contrast between damaged and undamaged regions in thermal images. The technique has previously shown to significantly reduce spatial image noise while maintaining defect contrast and preserving the important features of a flaw [6]. This is accomplished by a convolution of the data with a function containing a diffusion parameter. This parameter is high in regions of low gradients in image intensity and low in regions of high discontinuities in image intensity. For this data, the algorithm was applied to each frame of the data collected to remove spatial noise from the microbolometer data while maintaining any signal due to a delamination. Application of this algorithm resulted in a significant improvement in signal-to-noise of the final post-processed data, as seen below.

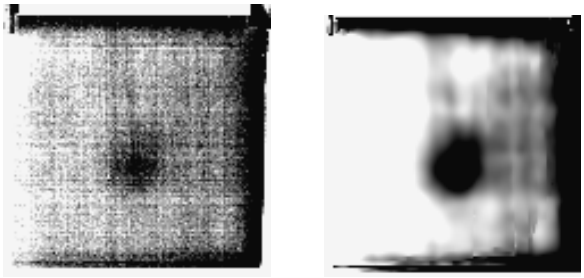

Figure 8. Post-processed microbolometer data, solar heating (A) without anisotropic diffusion, and (B) with Anisotropic Diffusion algorithm applied.

3.7. Frame rate

To minimize transfer time from camera memory to the internal compact flash card, the number of frames of data collected is critical. Reducing the number of frames stored can be accomplished by decreasing the frame rate or by decreasing the amount of time data is collected. Operationally, the crew must coordinate the start of data collection with the application of a shadowing source during the sequence and before the end of collection. For the DTO, this parameter was set at 60 seconds to ensure ample time for collection of the 10 second window after the initiation of shading.

Data was collected on impact panel number 8, and subsampled to obtain different effective frame rates. After applying the anisotropic diffusion algorithm and PCA during the first ten seconds after initiation of shading, a signal-to-noise analysis was performed to determine the loss in signal by decreasing the frame rate. The signal-to-noise is defined as the difference between the base material response and the flaw signal divided by the standard deviation of the base material. For the analysis, only the part of the image around the flaw area was used. The region used is shown in figure 9. A gaussian fit of the histogram was used to determine the normal and standard deviation in ~~of~~ the response of the base material. The histogram and its fit are shown in Figure 9. The lower shoulder was selected as the value for the flaw as shown in the Figure 9.

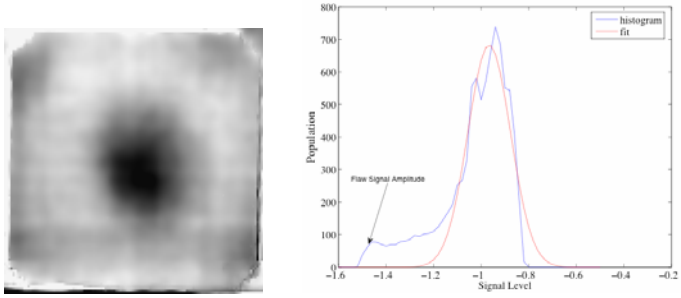

Figure 9. (A) Processed IR data for Impact Sample #8 (B) Histogram of processed IR image

As seen in the table below, a 30% loss in signal-to-noise occurs when reducing the frame rate to 1 Hz. For the DTO, data will be collected at 5 Hz for 60 seconds, resulting in a transfer time to the compact flash card of approximately 2 minutes.

Signal to Noise calculated for impacted specimen				
Reduction parameters Frequency of acquisition, start and stop channels	Signal	Standard Deviation Base Response	Signal to Noise	% Loss from 15 hz
15 Hz – 310,460	0.50	0.09	5.5	X
5 Hz - 104,154	0.50	0.09	5.5	0%
1 Hz – 21,31	0.39	0.10	3.9	29%
0.5 Hz – 10,15	0.34	0.10	3.4	38%
0.5 Hz – 11,16	0.37	0.10	3.6	34%

3.8. Vacuum

A custom made vacuum chamber was used (pictured in Figure 10) to quantify the effect on the measurement and detectability of defects for data taken in the vacuum of space. The vacuum chamber has three windows. Two quartz windows provide access for sample heating from an external source. Alternatively, incident heat flux on the samples can be accomplished with IR heaters placed inside the chamber and affixed to the interior of the front wall. The center window is germanium for viewing with the infrared camera. The maximum vacuum achievable is approximately 10^{-8}

torr. As can be seen in Figure 10, a vacuum provides a noticeable increase in defect detectability. At atmospheric pressure, air in the delamination does provide for some heat transfer across a boundary, even when the delamination between the composite layers is well defined. Being in a vacuum has the effect of making the boundary adiabatic.

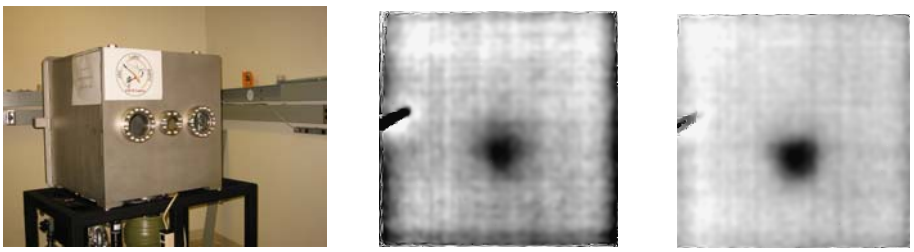

Figure 10. (A) Photograph of vacuum chamber (B) Panel #4 at atm (760 torr) (C) Panel #4 at vacuum (9x10-7 torr)

3.9. Radiation losses

A finite element simulation of the specimen with radiative heating and a periodically applied heat flux to the front, and with continuous radiative heat transfer into fixed temperature at the front and back surface was performed. A delamination was placed at the center plane of the specimen, with a radius to thickness ratio of 4:1. To reduce the computational time required for the simulation, the simulation was performed in cylindrical coordinates, and therefore assumes a circular delamination. For the simulations reported here, the back surface was assumed to always radiate into 270^{o}K and the front surface to radiate into either 10^{o}K or 170^{o}K. Simulations were also performed with incident fluxes of 1.1 Kwatt/meter^{2} and 0.55 Kwatt/meter^{2}. For all cases considered here, the incident flux is applied for the first half of a 90 minute cycle. All simulations assume an initial temperature of the entire specimen is 290 ^{o}K, with two full cycles of simulation before beginning to record the results. This was found to give results that were independent of the initial condition.

The time history of the temperature at a point far from the delamination is shown in figure 11. The time in the figure is set to be zero at the beginning of a cycle. The simulation indicates the temperature increases at the beginning of the cycle as the incident flux is applied. During the application of the incident flux, the temperature increases at a decreasing rate, asymptotically approaching a temperature that is determined by the point when the incident flux would be equal to the radiative heat transfer. This is seen in the figure where the case of radiative heat transfer into 170^{o}K. approaches a slightly higher temperature than for radiative heat transfer into 10^{o}K.

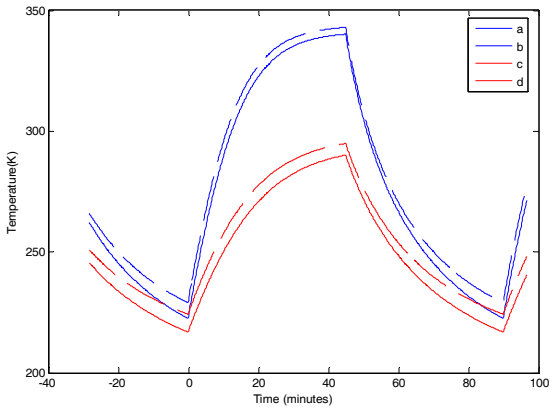

Figure 11– Results of simulation of thermal response of specimen radiating into two different temperatures and with two different surface fluxes. The individual plots are (a)– surface flux of 1.1 Kwatt/meter^{2}, radiating into 10^{o} K, (b) – surface flux of 0.55 Kwatt/meter^{2}, radiating into 10^{o} K, (c) – surface flux of 1.1 Kwatt/meter^{2}, radiating into 170^{o} K and (d) – surface flux of 0.55 Kwatt/meter^{2}, radiating into 170^{o} K.

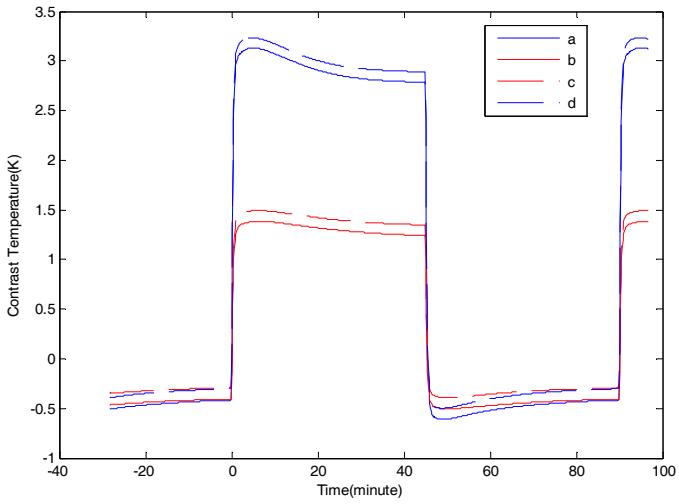

Figure 12– Contrast as a function to time based on simulation of thermal response of specimen radiating into two different temperatures and with two different surface fluxes. The individual plots are (a) – surface flux of 1.1 Kwatt/meter^2, radiating into 10^o K, (b) – surface flux of 0.55 Kwatt/meter^2, radiating into 10^o K, (c) – surface flux of 1.1 Kwatt/meter^2, radiating into 170^o K and (d) – surface flux of 0.55 Kwatt/meter^2, radiating into 170^o K.

For detection of the delamination, the important characteristic is the temperature difference between the delamination and an undamaged region. The temperature difference between the center of delamination and a reference point 5 times the radius away from the edge of the delamination is shown in figure 12. At the beginning of the cycle when the incident flux is applied, there is a rapid change in the temperature at the center of the delamination, relative to a reference point. This rapid change lasts for approximately 20 seconds when the most significant heat gradients are normal to the surface. Following this stage, the most significant gradients are in-plane, with the maximum contrast occurring as the in-plane heat flux reaches a quasi-static condition. As the temperature of the specimen continues to increase, the contrast decreases as the radiative heat transfer increases. It is important to note that the most significant factor in the contrast is the incident flux, not the temperature of the background being radiated into.

At the midpoint of the cycle, the incident flux becomes 0, and the radiative heat transfer begins to cool the specimen. The temperature difference decreases rapidly, with the most significant decrease occurring again within approximately 20 seconds. The absolute value of the temperature difference begins to decrease as the temperature of the specimen decreases. When the incident flux is zero, a state is reached where the temperature difference between the delaminated and undamaged regions depends on the difference in temperature between the temperature being radiated into by the front and back surfaces.

The time history of the spatial temperature profiles is shown in figure 13 at the beginning of the cycle. Time in the figure is referenced to the beginning of the cycle, corresponding to the application of incident flux. As can be seen in the figure, the contrast rapidly develops. It should also be noted that the best definition as to the extent of the delamination is considerably earlier than when the maximum contrast is obtained.

The temperature profile for different times at the midpoint of the cycle is shown in figure 14. This corresponds to the incident flux becoming zero with time given relative to the midpoint in the cycle. Again the profile changes rapidly with the temperature difference between the delamination and undamaged regions becoming negative within 45 seconds. The extent of the delamination is not as clearly defined in these profiles.

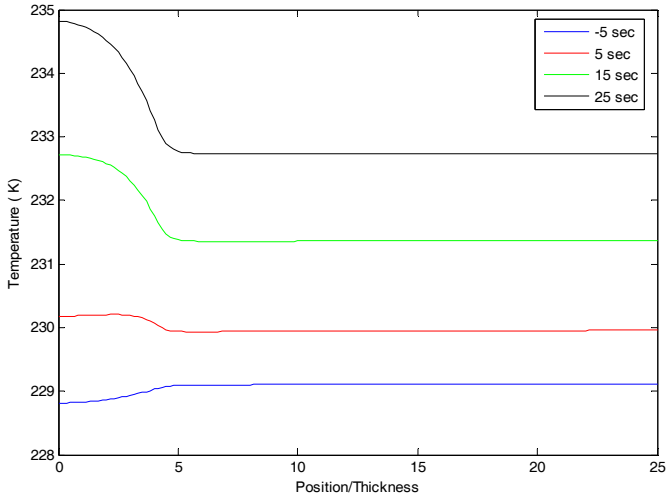

Figure 13. Temperature profile for different times based on simulation of thermal response of specimen radiating into 170°K different temperatures, with a surface flux of 1.1 Kwatt/meter^2. Time is relative to the start of application of the flux.

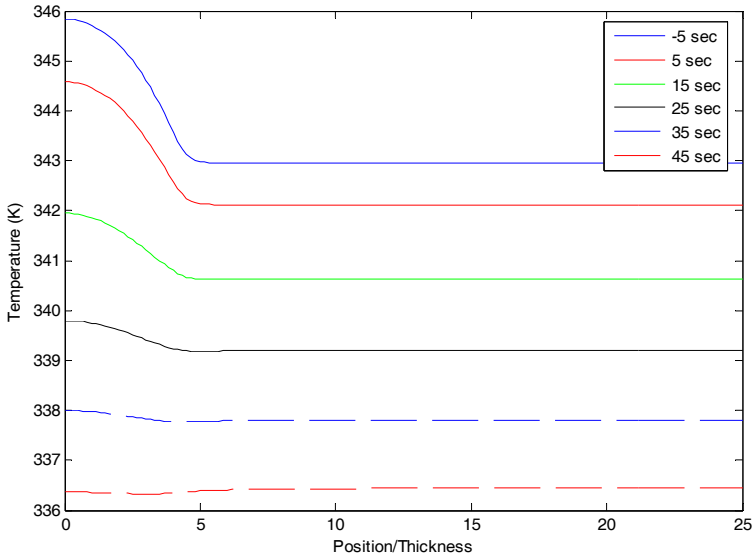

Figure 14– Temperature profiles for different times based on simulation of thermal response of specimen radiating into 170°K different temperatures, with a surface flux of 1.1 Kwatt/meter^2. Time is relative to the removal of the flux.

5. CONCLUSIONS

Significant progress has been made in inspection of the Shuttle's thermal protection system since the Columbia accident in February, 2003. In particular, advanced NDE techniques are being utilized for ground inspections between Shuttle missions. An experimental thermal NDE system has been developed for on-orbit inspection, leveraging those ground-based thermography techniques that have been used extensively for inspection of RCC. Changes to parameters critical

to the NDE measurement have been identified and investigated, and data analysis tools were modified to account for some of those variations.

The experimental IR EVA camera system is currently manifested on two Shuttle flights. Current mission plans include inspection of damaged RCC specimens on STS-121, currently scheduled for launch in September, 2005. The two NDE samples are mounted in a fixed Sample Box Assembly (SBA), along with samples that will be used to test RCC repair techniques. This provides an opportunity to image the NDE samples during a planned EVA. Additionally, a test article holder with two additional NDE samples will be flown on STS-121 and relocated to the International Space Station (ISS) to allow for additional data collection. On STS-121 and on STS-115, EVA timelines include procedures to image the WLE. The IR EVA team will support the DTO imagery on STS-121, the ISS EVA, and STS-115 from Mission Control.

Development of a space flight capable IR camera is an important asset as a potential tool for inspections of future exploration mission vehicle structures. The IR EVA Camera was heavily leveraged from existing technology and expertise based on extensive thermal NDE experience with ground inspections of RCC.

6. REFERENCES

1. Gehman, H., Adm. USN, Chairman, Columbia Accident Investigation Board Report, v3, US Gov. Printing Office document no. 033-000-01260-8, Aug. 2003.
2. Madaras, Eric I; Winfree, William P.; Prosser, William H.; Wincheski, Russell A.; and Cramer, K. Elliott, “Nondestructive Evaluation for the Space Shuttle’s Wing Leading Edge,” 41st AIAA/ASME/SAE/ASEE Joint Propulsion, Tucson, AZ, July 10-13, 2005.
3. Cramer, K. Elliott; Howell, Patricia A.; Madaras, Eric I,; Prosser, William P.; Wincheski, Russel; and Winfree, William P.,“Review of NDE Research and Development at NASA Langley Research Center in Support of the Space Shuttle Return to Flight,” Regional Congress on Non-Destructive and Structural Testing, 2005.
4. Gazarik, Michael; Johnson, Dave; Kist, Ed; Novak, Frank; Antill, Charles; Haakenson, David; Howell, Patricia; Jenkins, Rusty; Yates, Rusty; Stephan, Ryan; Hawk, Doug; and Amoroso, Michael, “Infrared On-orbit RCC Inspection with the EVA IR Camera: Development of Flight Hardware from a COTS System,” InfraMation: Infrared Camera Applications Conference, Las Vegas, NV, October, 2005.
5. Acknowledgements to Freeman Bertrand of Johnson Space Center for conducting impact tests at Southwest Research Institute.
6. Howell, Patricia A.; Zalameda, Joseph N.; and Winfree, William P., "Computational Analysis for Thermal NDE of Composites," SPIE 2003 conference on Optical Diagnostics for Fluids, Solids, and Combustion.